processes

MDPI

Article

Synthesis and Property Characterization of AM/AMPS/C18DMAAC/NVP Tetrameric Temperature-Sensitive Thickening Copolymer

Xu Chen [1,2,3], Xiangpeng Zhu [3], Cheng Gan [4], Yigang Li [5] and Diren Liu [1,2,*]

[1] College of Geophysics and Oil Resource, Yangtze University, Wuhan 430100, China; chenxu19890429@126.com
[2] Key Laboratory of Exploration Technologies for Oil and Gas Resources, Ministry of Education, Yangtze University, Wuhan 430100, China
[3] The Second Cementing Division, CNPC Bohai Drilling Engineering Company Limited, Tianjin 300280, China; 19902169627@163.com
[4] NO. 1 Drilling Engineering Company, CNPC Bohai Drilling Engineering Company Limited, Tianjin 300280, China; chenggan135@gmail.com
[5] CNPC Bohai Drilling Engineering Company Limited, Tianjin 300280, China; liyigang@cnpc.com.cn
* Correspondence: liudiren_yangtze@126.com

Abstract: The stability of cement slurries under high-temperature conditions poses a significant engineering challenge in cementing operations. This study explored the development of a novel tetrameric thermosensitive thickening polymer (TTSTC) as a solution to this problem. Aqueous free radical polymerization was employed to synthesize the polymer. The base monomers 2-acrylamido-2-methylpropanesulfonic acid (AMPS) and acrylamide (AM) were employed, in conjunction with the long-chain thermosensitive monomers octadecyldimethylallylammonium chloride (C18DMAAC) and N-vinylpyrrolidone (NVP). The optimal synthesis conditions were determined by orthogonal experiments as follows: monomer molar ratio (AM:AMPS:C18DMAAC:NVP) = 15:10:5:5, initiator concentration of 16 wt%, cross-linker concentration of 0.45 wt%, pH 6, and polymerization temperature of 60 °C. The chemical structure of TTSTC was characterized by Fourier transform infrared spectroscopy (FT-IR), proton nuclear magnetic resonance (1H-NMR), gel permeation chromatography, scanning electron microscopy, Zeta potential, and particle size measurement. The results verified the successful synthesis of the target polymer. Its thermal stability, thermosensitive thickening behavior, and salinity resistance were systematically investigated. Furthermore, the impact of TTSTC on the settling stability, rheological characteristics, and compressive strength of cement paste was assessed. The experimental findings demonstrated that TTSTC displayed noteworthy thermosensitive thickening properties at temperatures up to 279 °C, pH values ranging from 11 to 13, and $NaCl/CaCl_2$ concentrations between 0.05 and 0.5 g/L. The optimal performance of TTSTC was observed at mass fractions ranging from 0.6 to 0.8 wt%. When incorporated into the slurry at 0.6–1.0 wt%, TTSTC significantly improved the slurry settling stability, thickening properties, and 28d compressive strength at elevated temperatures compared with the control. When comparing the temperature-sensitive thickening performance of the newly developed treatment agent with that of the commercially available xanthan gum thickener, the results showed that for the cement slurry system containing the new treatment agent at a mass fraction of 0.6%, the reduction in consistency was 30.9% less than that of the cement slurry system with xanthan gum at a mass fraction of 0.6%. These findings indicate that TTSTC has the potential to function as a highly effective additive in cementing operations conducted in extreme environments, thereby enhancing the stability and dependability of such operations.

check for updates

Academic Editors: Navid Aslfattahi, Kumaran Kadirgama, Lingenthiran Samylingam and Mohammad Reza Chalak Qazani

Received: 11 February 2025
Revised: 2 March 2025
Accepted: 4 March 2025
Published: 20 March 2025

Citation: Chen, X.; Zhu, X.; Gan, C.; Li, Y.; Liu, D. Synthesis and Property Characterization of AM/AMPS/C18DMAAC/NVP Tetrameric Temperature-Sensitive Thickening Copolymer. *Processes* **2025**, *13*, 922. https://doi.org/10.3390/pr13030922

Copyright: © 2025 by the authors. Licensee MDPI, Basel, Switzerland. This article is an open access article distributed under the terms and conditions of the Creative Commons Attribution (CC BY) license (https://creativecommons.org/licenses/by/4.0/).

Keywords: temperature-sensitive thickening polymers; cementing water slurries; aqueous solution radical polymerization; performance characterization

1. Introduction

In the context of oil production, the cementing process entails a progressive increase in well depth, which is accompanied by a discernible upward trend in bottom-hole temperature. This phenomenon poses a significant challenge to the stability of the cement slurry system [1–4].

At elevated temperatures, the Brownian motion of particles in the cement slurry becomes more active. This heightened activity disrupts the internal viscous force equilibrium of the cement slurry, ultimately resulting in its settlement and instability [5]. This phenomenon has the potential to compromise the integrity of the cementing process, thereby compromising its quality. In extreme cases, it can also pose a safety hazard during the drilling of oil and gas wells, potentially resulting in well collapse and oil and gas leakage [6], posing a significant risk to oil production operations.

Under high temperature conditions, conventional cement slurry stabilizers often exhibit the phenomenon of "high-temperature thinning" [7]. Under high-temperature conditions, they are unable to effectively inhibit the settling of particles in the cement slurry, and it is difficult to ensure the stability of the cement slurry. Therefore, the exploration of a novel cement slurry additive suitable for high-temperature conditions has become the focus of research. In recent years, thermosensitive thickening polymers have increasingly become a research focus to address this issue due to their distinct thermosensitive thickening properties.

Thermosensitive thickening polymers are a special class of polymeric materials. In a given temperature range, the viscosity of their solutions exhibits an upward trend with increasing temperature [8]. This distinctive property of the polymer is evident in its temperature-dependent behavior, wherein an increase in temperature results in a concomitant increase in solution viscosity within the specified temperature range [9,10]. An increase in temperature has been shown to induce a phase transition within the thermosensitive groups, thereby exposing additional hydrophobic groups. An increase in temperature has been shown to induce a phase transition within the thermosensitive groups, thereby exposing additional hydrophobic groups. This augmented hydrophobic interaction promotes the cross-linking of polymer molecular chains, leading to the formation of a three-dimensional spatial network structure. Consequently, the viscosity of the solution undergoes a substantial increase, thereby impeding the sedimentation of cement slurry particles to a considerable extent [11].

To date, researchers have conducted exhaustive studies on a variety of thermosensitive thickening polymers and obtained specific results [12–14]. A significant amount of research has been devoted to the study of poly(N-isopropylacrylamide) (PNIPAM) and its derivatives due to their distinctive critical solution temperature at the lower end behavior [15–17]. Nevertheless, PNIPAM has certain drawbacks, including a limited thermosensitive range and inadequate salt resistance, which limit its applicability in complex environments [18]. A number of studies have sought to modify the material by introducing different monomers. However, it remains challenging to meet the stringent industrial requirements [19,20]. Therefore, the development of a thermosensitive thickening copolymer with easy synthesis and excellent performance is of great practical importance.

In this study, a quaternary temperature-sensitive thickening copolymer (TTSTC) of AM/AMPS/C18DMAAC/NVP was designed and synthesized [21]. The limitations of

traditional temperature-sensitive thickening systems were overcome through the synergistic effect of multifunctional monomers. The long-chain carbon structure of C18DMAAC enhanced the hydrophobic association ability, addressing the issue of insufficient physical cross-linking in traditional systems at high temperatures. The sulfonic acid groups of AMPS provided excellent salt and calcium resistance, as well as the ability to adsorb on cement particles, overcoming the defect of traditional thickeners failing in complex ionic environments. The cyclic structure of NVP improved thermal stability and enabled precise regulation of the temperature-sensitive response, solving the problem of short-lived thickening effects at high temperatures. AM, as the backbone monomer, provided the necessary water solubility and chain flexibility. This molecular design strategy offers a more reliable rheological property control scheme for high-temperature deep-well cement slurry systems.

Through the orthogonal experimental design, the ratio composition of each monomer was systematically screened and optimized. By integrating the unique advantages of different monomers, a polymer material with a wide temperature-sensitive range, excellent thickening performance, and outstanding salt and alkali resistance was prepared to meet the needs of oil exploitation scenarios.

2. Experimental Design

2.1. Experimental Raw Materials

Analytical-grade acrylamide (AM) was obtained from Sinopharm Chemical Reagent Co., Ltd. (Shanghai, China). Chemically pure 2-Acrylamido-2-methylpropanesulfonic acid (AMPS) was sourced from Guangdong Wengjiang Chemical Reagent Co., Ltd. (Wengjiang, China). Similarly, chemically pure N-Vinylpyrrolidone (NVP) was acquired from Guangdong Fangxin Biotechnology Co., Ltd. (Fangxin, China). Analytical-grade N,N-dimethyloctadecyl tertiary amine (C18DMA) was furnished by Guangdong Wengjiang Chemical Reagent Co., Ltd. Allyl chloride (C_3H_5Cl), in a chemically pure grade, was obtained from Aladdin Chemical Reagent Co., Ltd. (Shanghai, China). Analytical-grade ammonium persulfate (APS) was sourced from Tianjin Jiangtian Chemical Technology Co., Ltd. (Tianjin, China), while analytical-grade sodium bisulfite ($NaHSO_3$) was procured from Tianjin Guangfu Technology Development Co., Ltd. (Tianjin, China). Analytical-grade sodium hydroxide (NaOH) was also obtained from Sinopharm Chemical Reagent Co., Ltd., as was the analytical-grade absolute ethanol. Deionized water was generated within the laboratory setting; Xanthan gum, industrial purity, was provided by Zhengzhou Pure Chemical Products Co., Ltd. (Zhengzhou, China).

2.2. Polymer Synthesis Process

In this study, C18DMAAC was first synthesized using C18DMA and C_3H_5Cl, and then aqueous solution radical polymerization of AM, AMPS, C18DMAAC, and NVP was performed to produce a four-component thermosensitive thickening copolymer (TTSTC). The specific work included the following steps:

(1) Synthesis of C18DMAAC

① To dissolve and prepare the reaction system, 100 milliliters of acetonitrile was used to dissolve 29.7 g of C18DMA. The resulting solution was then transferred to a 250 milliliter three-necked flask to establish the reaction system. To ensure that the temperature of the reaction remained within the desired range of 0–5 °C, the flask was immersed in an ice bath.

② For chloropropene dropwise addition, 9.2 g of C_3H_5Cl was slowly added dropwise under ice bath conditions, controlling the drop rate to ensure that the reaction temper-

ature remained stable between 0–5 °C. Stirring was continued during the dropwise addition to ensure uniform mixing of the reactants.

③ For temperature increase and reaction, upon completion of the addition, the ice bath was removed, the reaction temperature was raised to 45 °C, and stirring was continued for 24 h. The temperature was monitored throughout the reaction to ensure that it did not exceed 45 °C to prevent side reactions or overreactions.

④ For solvent removal, when the reaction was complete, vacuum distillation was used to remove the acetonitrile solvent and concentrate the reaction product. This process was performed under mild conditions to avoid decomposition of the product.

⑤ For recrystallization, a quantity of 200 milliliters of anhydrous ether was used to dissolve the crude product, which was then recrystallized. This step helped to remove unreacted raw materials and by-products. The recrystallized solid was separated by suction filtration, washed, and collected.

⑥ For drying, to ensure the complete drying of the product and the removal of the residual solvent, the recrystallized solid product was placed in a vacuum drying oven and dried under vacuum at 40 °C for 12 h.

Through this process, the white solid C18DMAAC was finally obtained.

(2) Synthesis of TTSTC

① For the preparation of monomer solution, AM, AMPS, and NVP were dissolved in 80 mL of deionized water, and C18DMAAC was dissolved separately in 20 mL of deionized water; 20% by mass NaOH was added, and the pH was adjusted to 6.0~7.0.

② For the reactor preparation, a 250 mL four-port flask equipped with a mechanical stirrer, thermometer, nitrogen gas line, and dropping funnel was placed in a water bath.

③ For the reaction procedure, the monomer solution was added to the reactor, nitrogen was introduced to the deoxygenate for 30 min, the temperature was raised to 50 °C, the freshly prepared $(NH_4)_2S_2O_8$ and $NaHSO_3$ solution (1.2:1) was quickly added, and it was reacted at 50 °C for 6 h at a stirring rate of 300 rpm.

④ Post-treatment, upon completion of the reaction, the product solution was transferred to an excess of acetone, resulting in precipitation of the target compound. The precipitate was then collected, thoroughly washed three times with acetone, and dried under vacuum at 40 °C for 24 h. This process was repeated until a consistent weight was achieved, resulting in a white powdered temperature-sensitive thickening polymer. As shown in Figure 1, the polymerization grafting process was characterized by the following molar ratios: X, Y, Z, and M, corresponding to AM, AMPS, C18DMAAC, and NVP, respectively.

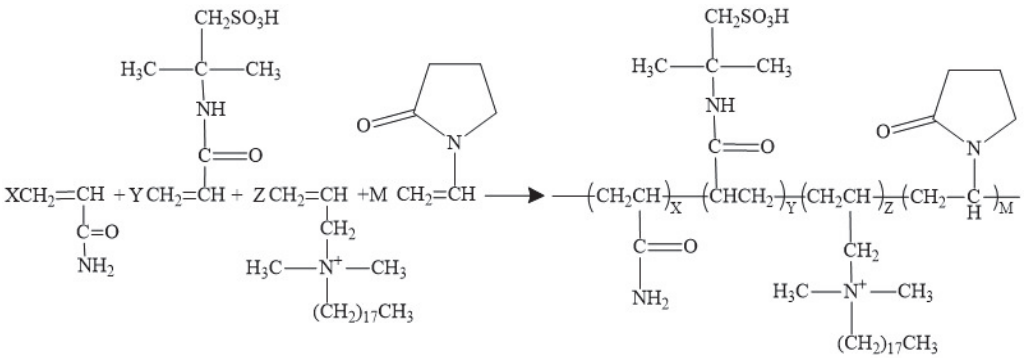


Figure 1. TTSTC's grafting technology route.

2.3. Synthesis Conditions Optimization

According to the principle of free radical polymerization, the properties of copolymers were mainly affected by multiple factors, including the molar ratio of monomers X:Y:Z:M (r), the mass fraction of monomers (w_1), the mass fraction of the initiator [22] (w_2), the pH of the reaction system (pH), and the reaction temperature (T). The properties of the copolymer were significantly influenced by the variable values of these factors. Consequently, an orthogonal test comprising five factors and four levels was developed, as illustrated in Table 1.

Table 1. Orthogonal experiment factor level table.

Levels	Factors				
	r	w_1 (%)	w_2 (%)	pH	T (°C)
1	10:15:5:5	10	0.40	5	40
2	15:10:5:5	13	0.45	6	50
3	13:13:6:3	16	0.50	7	60
4	13:13:3:6	19	0.55	8	70

Based on the above factors and levels, an L16(4^5) orthogonal test table was constructed as shown in Table 2. The evaluative metric that was adopted was the density disparity between the upper and lower layers of the generated cement slurry. In the experiment, it was observed that as the density difference decreased, the stability of the corresponding cement slurry increased. The cement slurry system in this paper was as follows: G-grade cement and quartz sand with a particle size of 100–140 mesh used in conjunction with it, retarder (the dosage was 0.4%), filter loss agent (dosage was 4%), suspending agent (dosage was 0.5%), and defoamer. The density of the system formed by the above materials was 1.92 g/cm^3. The test conditions for cement paste curing were as follows: temperature, 120 °C, and pressure, 20.7 MPa. As illustrated in Table 2, the factors that were identified as contributing to the stability of cement slurry, in order of importance, were as follows: r > w_1 > pH > T > w_2. The optimal synthesis conditions were as follows: r = 15:10:5:5, w_1 = 16%, w_2 = 0.45%, pH = 6, and T = 60 °C. The corresponding parameters in Section 2.2 were adjusted to the preferred parameters in this section for subsequent analysis.

Table 2. Orthogonal experiment table.

No	r	r	w_1 (%)	w_2 (%)	pH	T (°C)	Density Difference (g/cm^{-3})
T1	1	1	1	1	1	1	0.194
T2	1	1	2	2	2	2	0.128
T3	1	1	3	3	3	3	0.113
T4	1	1	4	4	4	4	0.203
T5	2	2	1	2	3	4	0.177
T6	2	2	2	1	4	3	0.164
T7	2	2	3	4	1	2	0.107
T8	2	2	4	3	2	1	0.13
T9	3	3	1	3	4	2	0.211
T10	3	3	2	4	3	1	0.181
T11	3	3	3	1	2	4	0.123
T12	3	3	4	2	1	3	0.135
T13	4	4	1	2	2	3	0.235
T14	4	4	2	1	1	4	0.247
T15	4	4	3	4	4	1	0.252
T16	4	4	4	3	3	2	0.256
K_1	0.160	0.160	0.204	0.182	0.171	0.189	
K_2	0.145	0.145	0.180	0.169	0.154	0.176	
K_3	0.163	0.163	0.149	0.178	0.182	0.162	
K_4	0.248	0.248	0.181	0.186	0.208	0.188	
R	0.103	0.103	0.056	0.017	0.054	0.028	

Here, K_i represents the average response value of factor i at different levels; R represents the magnitude of the response difference among various levels of the factor, reflecting the degree of influence of the factor on the experimental results. The larger the R value, the more significant the influence.

2.4. Characterization of Polymers

The chemical structure of the polymers was analyzed in detail by Fourier transform infrared spectroscopy (FT-IR) using a NEXUS FT Fourier transform infrared spectrometer (Thermo Nicolet, Madison, WI, USA). The procedure was as follows: a dry polymer sample was thoroughly mixed with KBr, and the mixture was uniformly dispersed during grinding before being pressed into a tablet. The pressed tablet was used as the test sample. The scanning range was set to 400–4000 cm^{-1}. During operation, the instrument could effectively identify the chemical bonds and functional groups contained in the polymer, thereby determining its chemical structure, by accurately detecting and analyzing characteristic absorption peaks at different wave numbers.

The ^1H NMR analysis used a Bruker AVANCE III HD (Zurich, Switzerland) nuclear magnetic resonance spectrometer and deuterated water as a solvent to perform ^1H NMR tests on the polymer. When the polymer molecule was in a strong magnetic field, hydrogen atoms in different chemical environments produced specific resonance frequencies that were reflected as different chemical shifts in the spectrum. By carefully analyzing these chemical shifts, information such as the type and number of hydrogen atoms and their relative positions in the molecule could be obtained, further confirming the structure of the polymer and providing an important basis for a deeper understanding of the microscopic structure of the polymer.

Gel permeation chromatography (GPC) analysis was carried out using the Shimadzu GPC-20A system (Kyoto, Japan) and the SB-806M HQ aqueous column (Tokyo, Japan). A 0.1 mol/L NaCl solution was used as the mobile phase, and the GPC analysis was performed at 40 °C and 1.7 MPa. Polyacrylamide was used as the molecular weight standard. The dried and purified samples were dissolved in the mobile phase at a mass fraction of 1% and then subjected to instrumental testing.

The microstructure of the polymer TTSTC was observed using cryo-scanning electron microscopy (Cryo-SEM). First, a certain amount of TTSTC was magnetically stirred and dissolved in a 60 °C constant-temperature water bath for 48 h. It was fixed on the sample holder with cryo-glue and then rapidly frozen with liquid nitrogen. Through a cryo-fracture instrument, brittle fracture was carried out at −140 °C in a vacuum environment of 10^{-4} mbar, followed by sublimation drying at −90 °C for 2 h and platinum/carbon conductive layer evaporation plating treatment. Finally, the micro-morphology was observed using a Quanta 250 FEG electron microscope (Hillsborough, FL, USA) at a low temperature of −100 °C, at an acceleration voltage of 15 kV, and in a low-vacuum mode.

The Zeta potential and dynamic light scattering particle size of the prepared polymer solution were measured using a Nano ZS nanoparticle size and Zeta potential analyzer produced by Malvern Instruments Ltd.(Malvern, UK). First, a polymer with a mass fraction of 0.6% was dissolved in deionized water to prepare a homogeneous solution. The Zeta potential and particle size of this solution were measured at 20–80 °C.

2.5. Polymer Property Testing

For thermogravimetric analysis (TGA), the thermal stability of polymers was scientifically evaluated using a NETZSCH STA449F5 simultaneous thermal analyzer (Selby, Germany). For the test, a sample of approximately 10 mg was accurately weighed, and a temperature range of 30 °C to 600 °C was set. In the experiment, N_2 was used as the protective gas at a flow rate of 30 mL/min. The temperature was raised at a constant

rate of 10 °C/min. This was done to prevent unwanted side reactions such as oxidation of the sample during the heating process. Throughout the test, the instrument recorded the change in sample mass with temperature in real time. By analyzing the thermogravimetric curve, the thermal decomposition behavior of the polymer at different temperature ranges could be determined and its thermal stability evaluated. This provided key data for evaluating the thermal performance of polymers in various application scenarios.

For the temperature-sensitive thickening performance test, first, the polymer was meticulously formulated into a series of aqueous solution samples, each with different concentrations. Then, the apparent viscosity of the aqueous polymer solution (0.2%, 0.4%, 0.6%, and 0.8%) at different weight fractions was accurately measured at different temperatures using a HAAKE RS1 Advanced Rheometer. The temperature range set for this test was 20 °C to 200 °C. Within this range, the temperature was increased at a constant rate of 2 °C/min while maintaining a shear rate of 511 s^{-1}. This was done to comprehensively characterize the rheological properties of the aqueous polymer solution at varying temperatures and to elucidate the principle underlying temperature-dependent and temperature-sensitive thickening performance.

To investigate the effect of salt ions on the temperature-sensitive thickening property of the polymer, a salt tolerance experiment was conducted. In the experimental procedure, a series of polymer solutions containing different concentrations of NaCl were carefully prepared. The NaCl concentrations were set at 0.05 g/L, 0.2 g/L, 0.5 g/L, and 3 g/L. The apparent viscosity of these polymer solutions with different salt concentrations was measured at different temperatures using a rheometer. By comparing and analyzing the viscosity data under different salt concentrations and temperature conditions, the interaction mechanism between salt ions and polymers was analyzed in depth, and the influence of salt ions on the temperature-sensitive thickening performance of polymers was revealed.

Alkali resistance tests were performed with a focus on studying the stability of polymers in an alkaline environment. The pH of the aqueous polymer solution was carefully calibrated to specific values between 11 and 14 by incrementally adding precise amounts of NaOH. The apparent viscosity of the polymer solutions was measured using a rheometer at various pH values and temperatures. The stability of the polymer in an alkaline environment could be evaluated by analyzing the viscosity changes under different conditions and temperatures. At the same time, the effect of the alkaline environment on the structure and properties of the polymer could be determined, and a theoretical basis for the alkaline environment encountered by the polymer in practical applications could be provided.

2.6. Testing the Effect of Polymers on the Properties of Cement Paste

The cement slurry was first prepared according to the procedure described in Section 2.3. The prepared slurry sample was then transferred to the HTD7322 autoclave (Shanghai, China). The unit was activated, and the temperature was gradually increased until it reached 120 °C. The slurry was then stirred continuously at this temperature for 40 min. This was done to ensure homogeneity and stability of the slurry system. A gradual cooling process was then initiated. Once the temperature was reduced to 60 °C, stirring was stopped, and a slurry sample was collected. The substance was first transferred to a sedimentation tube. The sedimentation tube was then placed in a high-temperature, high-pressure autoclave. The temperature of the autoclave was set at 110 °C, and the cement slurry was exposed to this temperature until it was completely set.

Once the setting process was complete, the sedimentation tube was removed, and the densities of the upper and lower portions of the cement paste inside the tube were accurately measured to calculate the density discrepancy. This density discrepancy could directly indicate the settling stability of the cement paste during high-temperature and high-pressure curing.

Based on the above-mentioned testing work, with the addition of a commercial xanthan gum thickener at a mass fraction of 0.6% as a control, the consistency changes of cement slurries without thickener, with 0.6% mass fraction of TTSTC, and with 0.6% mass fraction of xanthan gum under different temperature and pressure conditions were recorded in detail. The influence law of polymers on the consistency of cement slurries was analyzed in depth. The DYE-300S model compression and flexure tester (Wuxi, China) was used to apply axial pressure to the final cement paste sample. According to the data collected by the instrument, the compressive strength of the cement paste was accurately determined to thoroughly investigate the effect of the polymer on the compressive strength of the cement paste.

The influence of polymer additives on the cement slurry in 2.3 was investigated using a YT12959-08 type heat of hydration tester (Wuxi, China). First, the constant-temperature box of the instrument was set to 20.00 ± 0.02 °C, and self-calibration was completed within 24 h. Exactly 500 g of cement was precisely weighed and mechanically mixed with a fixed amount of additives for 3 min. Then, using an OWC-2000D stirrer (Shanghai, China), water was added rapidly at a liquid-to-solid ratio of 0.44 and stirred at a rotational speed of 4000 ± 200 r/min for 10 s to prepare the slurry. After the slurry was poured into a calorimeter bottle purged with nitrogen, a thermocouple was immediately installed, and the bottle was sealed. The bottle was then placed in the constant-temperature box and continuously monitored at 20.00 ± 0.02 °C for 90 h. Data were recorded every 1 min.

3. Results and Discussion

3.1. Structural Characterization of the Polymers

3.1.1. FT-IR Analysis Results

In Figure 2, the FT-IR spectrum shows that the broad and intense absorption peak around 3300–3500 cm^{-1} could be attributed to the N–H stretching vibration of the amide moiety (-$CONH_2$) in the AM monomer [23]. This result indicated that AM was successfully involved in the polymerization reaction. The absorption peak within the range of 1660–1680 cm^{-1} was attributed to the C=O stretching vibration of the amide group [24], further confirming the presence of the AM unit. The S=O stretching vibration of the sulfonic acid group (-SO_3H) in AMPS was represented by the characteristic absorption peaks at 1211 cm^{-1} and 1092 cm^{-1} [25], indicating that the AMPS monomer had also been incorporated into the copolymer molecular chain. The absorption peaks at 2839–2902 cm^{-1} were attributed to the characteristic vibrations of methyl and methylene [26], indicating that this monomer was involved in the polymerization reaction. In addition, the absorption peak at 1658 cm^{-1} was attributed to the C=O stretching vibration of the pyrrolidone ring in NVP [27], proving that the NVP monomer was also polymerized into the copolymer. The presence of these distinctive absorption peaks in the figure, along with the disappearance of the characteristic C=C signal, provided compelling evidence that AMPS, C18DMAAC, AM, and NVP were effectively polymerized to generate the desired quaternary copolymer.

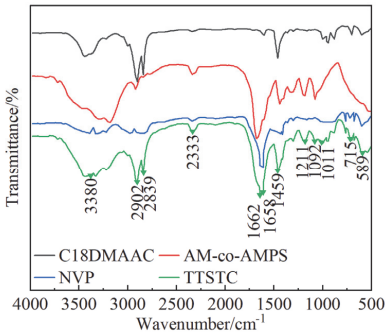


Figure 2. FT-IR of C18DMAAC, AM-co-AMPS, NVP, and TTSTC in this study.

3.1.2. ^{1}H NMR Analysis Results

In the study of the target copolymer structure, ^{1}H NMR spectroscopy was used to accurately characterize it. By analyzing the signal peaks in the spectrum (Figure 3), the structural characteristics of the copolymer could be clearly inferred from the order of chemical shifts (δ) from low to high.

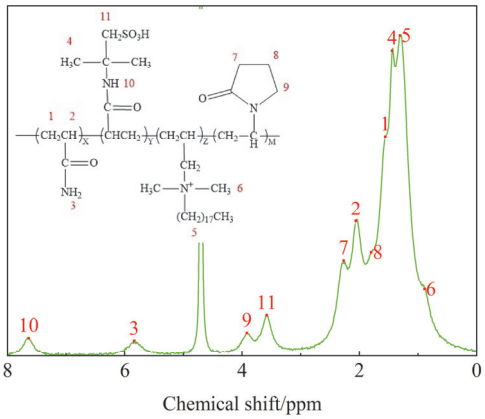


Figure 3. H NMR spectrum (D_2O, 20 °C) of TTSTC solutions.

Initially, the peak at δ = 0.88 ppm was associated with the proton signal of the terminal methylene (-CH_3) group in C18DMAAC, indicating that the copolymer contained C18DMAAC units. The strong peak at δ = 1.288 ppm was attributed to the characteristic absorption of the -$(CH_2)_{16}$- group in the C18 long chain [28], further confirming the presence of the C18 long chain. As the chemical shift increased, the signals at δ = 1.57 ppm and δ = 2.04 ppm [23] came from the methylene (-CH_2-) and methylene (-CH-) protons on the main chain of each monomer, respectively, revealing the basic structural units of the copolymer main chain.

In the higher chemical shift region, δ = 3.58 ppm was the signal of the -CH_2 proton in AMPS [29], and the signals at δ = 3.92 ppm, 2.23 ppm, and 1.91 ppm were attributed to the -CH_2 protons in NVP [30], confirming the involvement of AMPS and NVP monomers. In addition, the characteristic peaks of -NH- of AMPS and -NH_2 of AM were observed at δ = 7.65 ppm and δ = 5.83 ppm, respectively, which further complemented the structural information of each monomer in the copolymer.

In particular, the absorption peaks of C=C (δ = 6.15 ppm and δ = 4.59 ppm) completely disappeared. Since the C=C double bond was the active site of the monomer participating in the polymerization reaction, the disappearance of its absorption peak indicated that the double bond had completely participated in the reaction, thus providing strong evidence for the successful synthesis of the target copolymer and that the reaction was sufficient, with no unreacted double bonds present.

3.1.3. Gel Permeation Chromatography Analysis Results

The GPC test results in Figure 4 indicated that the TTSTC polymer exhibited a wide elution time distribution, suggesting a broad molecular weight distribution and non-uniformity in the length of polymer chains. The number-average molecular weight (M_n) was 1,462,844, and the weight-average molecular weight (M_w) was 2,955,412. The molecular weight reached the million level, which was in line with the characteristics of high-molecular-weight materials. The dispersity index (DI) was 2.02, further reflecting the significant differences in polymer chain lengths.

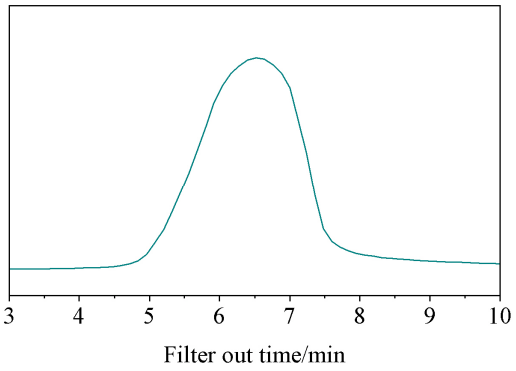


Figure 4. Test results of polymer by gel permeation chromatography.

The molecular weight of the polymer had a crucial impact on its thermosensitive thickening performance. A larger molecular weight enhanced the thickening effect of the polymer during temperature changes, which was consistent with the high-molecular-weight characteristic of the TTSTC polymer. Meanwhile, the relatively wide molecular weight distribution (DI = 2.02) implied that different segments of the polymer chains responded at different rates to temperature changes. This may lead to non-uniformity in the thickening effect within certain temperature ranges. However, the characteristic of a wide distribution also endowed the polymer with adaptability under different temperature conditions, enabling it to have a relatively broad range of thickening responses.

During the synthesis process, the TTSTC polymer successfully achieved a high molecular weight and possessed the characteristics required for thermosensitive thickening. The wide molecular weight distribution provided diversity and flexibility to its thickening performance at different temperatures, meeting the design requirements of thermosensitive thickening materials.

3.1.4. Scanning Electron Microscopy Analysis Results

Figure 5 presents the microstructure of a 0.6% (mass fraction) TTSTC solution observed by cryo-scanning electron microscopy. A thorough analysis of this microstructure revealed that when the mass fraction of the TTSTC solution reached the specific concentration of 0.6%, intermolecular cross-linking and association occurred among the polymer molecules in the solution. Consequently, a spatial network structure was formed. This unique spatial network structure was the key factor endowing the TTSTC solution with a high viscosity.

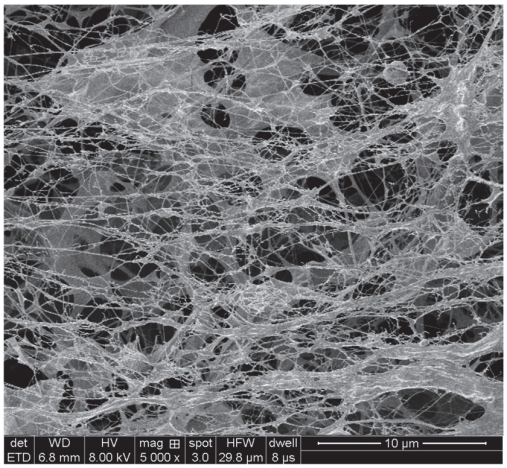


Figure 5. Cryo-scanning electron microscopy of 0.6% TTSTC solution.

3.1.5. Zeta Potential and Hydrated Dynamic Diameter of Polymer Analysis Results

Figure 6 illustrates the variation laws of Zeta potential and hydration radius in 0.6% TTSTC aqueous solution at different temperatures. As can be seen from the figure, with the increase in temperature, the hydrated particle size of the polymer showed an increasing trend, with the particle size range being 1365–2423 nm. The absolute value of the Zeta potential also increased with the rise of temperature, with the minimum value being 36 mV. The temperature range of 40–60 °C was the interval where the changes in Zeta potential and hydrated particle size were most significant, indicating that within this temperature range, the polymer exhibited obvious thermosensitive characteristics, which may be due to the conformational changes of the polymer chains or the enhancement of hydrophobicity. After exceeding 60 °C, the changes in the hydrated particle size and Zeta potential tended to level off, suggesting that high temperature had a relatively small impact on the further changes of the polymer. The prepared TTSTC polymer maintained good thermosensitivity, dispersibility, and stability throughout the entire temperature range.

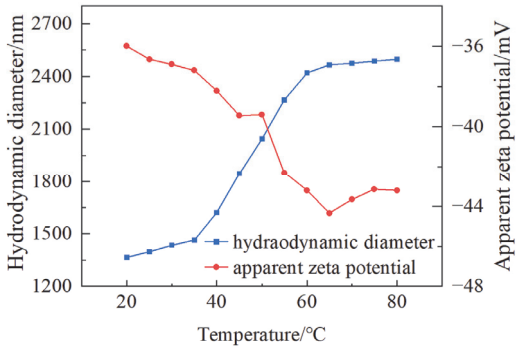


Figure 6. The Zeta potential and hydrodynamic diameter of TTSTC solutions at various temperatures.

3.2. Properties of Polymers

3.2.1. Thermogravimetric Analysis

As can be seen from the TG/DTG curve (Figure 7), there was a small mass loss step of the copolymer in the range of 50–150 °C, which was mainly due to the moisture adsorbed by the copolymer and the volatilization of a small amount of low-boiling impurities. As the temperature elevated further, reaching between 279 and 346 degrees Celsius, the copolymer exhibited a substantial mass loss. This phenomenon corresponded to the pronounced peak in the derivative thermogravimetric (DTG) curve within this temperature range. This was the stage at which thermal decomposition of the copolymer molecular chain began. This stage of decomposition was mainly due to the possible deamination reaction of the amide group in the AM unit at high temperatures, which caused the molecular chain to break. The sulfonic acid group in AMPS may also decompose at high temperatures, producing gases such as sulfur dioxide. Among these, at a temperature of about 316 °C, the degree of decomposition reached its most violent state, which in turn led to significant mass loss at this stage. At 346–450 °C, the main chain of TTSTC began to break, and the molecule gradually decomposed. When the temperature exceeded 450 °C, the rate of mass loss of the copolymer gradually slowed down, but there was still a continuous mass loss until around 600 °C, when the mass remained basically stable. At this time, the remaining residue was mainly composed of some inorganic components and carbides that were difficult to completely decompose.

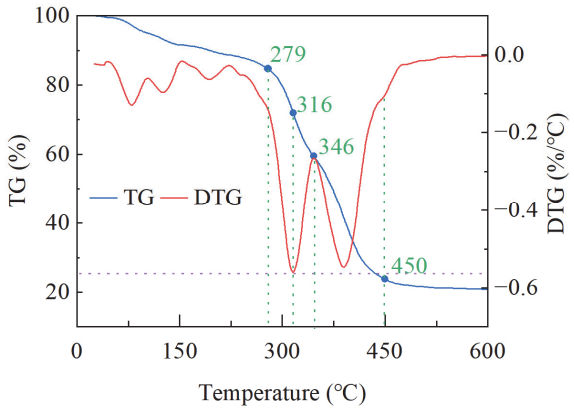


Figure 7. TG/DTG curves of TTSTC solutions.

In this study, the copolymer's initial decomposition temperature was measured at 279 °C. This finding suggested that below this temperature threshold, the copolymer maintained a relatively stable internal molecular arrangement. This was because both the pyrrolidone ring and the long-chain alkyl group possessed a certain degree of rigidity. They were capable of enhancing the rigidity of the polymer molecular chain, thereby enabling the polymer to maintain a stable structure at high temperatures. The maximum decomposition rate temperature was 316 °C, indicating that at this temperature, the decomposition reaction of the copolymer was the most severe; the residual carbon rate was about 20%. The aforementioned results demonstrated that the copolymer exhibited favorable thermal stability, with the capacity to preserve a relatively stable structure at temperatures below 279 °C.

3.2.2. Temperature-Sensitive Thickening Properties

An extensive analysis of the change in apparent viscosity of the polymer solution with temperature was performed at TTSTC. The mass fractions used in this analysis were 0.2%, 0.4%, 0.6%, and 0.8%. As shown in Figure 8, the specific results were obvious. As can be clearly seen from the figure, as the mass fraction of TTSTC was gradually increased, the initial apparent viscosity of the polymer solution exhibited a regular variation, reaching values of 94.2 MPa·s, 119.7 MPa·s, 138.9 MPa·s, and 156.8 MPa·s.

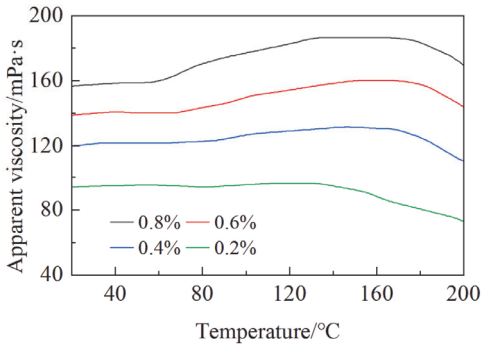


Figure 8. The thermosensitive thickening properties of solutions with different mass fractions of TTSTC solutions.

When the mass fraction of TTSTC stood at 0.2%, the apparent viscosity of the polymer solution remained relatively constant until the temperature reached 134 °C. Nevertheless, when the temperature surpassed 134 °C, the concentration dropped, and the apparent viscosity declined. As the mass fraction was elevated to 0.4%, the apparent viscosity maintained a relatively constant value until it reached 80 °C. Between 80 °C and 150 °C, the apparent viscosity of the solution tended to increase, and above 150 °C, the viscosity began to decrease. For a mass fraction of 0.6%, the viscosity shown by the polymer solution

remained stable until 75 °C. Between 75 °C and 160 °C, the viscosity gradually increased. When the temperature went beyond 160 °C, the viscosity began to decrease. As the TTSTC mass fraction approached 0.8%, the apparent viscosity remained relatively constant until it reached 65 °C. However, between 65 °C and 165 °C, there was a substantial increase in viscosity. Furthermore, when the temperature exceeded 165 °C, the viscosity began to decrease. It is worth noting that when the TTSTC mass fraction was 0.6% and 0.8%, even when the temperature reached 200 °C, the apparent viscosity was still not lower than the apparent viscosity at 20 °C.

An examination of the experimental outcomes disclosed considerable differences in the mechanism of polymer thickening at low mass fractions of 0.2% and 0.4% and high ones of 0.6% and 0.8%.

At low mass fractions, the polymer molecules were more dispersed in the solution, and the distance between the molecules was larger (Figure 9a–c). In terms of molecular structure, AM, as a hydrophilic monomer, endowed the molecular chain with solubility in water due to its own chemical structure, which allowed the molecular chain to exist more freely in the solution. However, due to the large distance between the molecules, there were only a small number of weak interactions such as hydrogen bonds between the molecules, which made it difficult to form an effective intermolecular connection network [19]. AMPS was also strongly hydrophilic, which further enhanced the dispersion of the molecular chains in water, making the molecular chains more flexible. However, this also meant that the molecular chains lacked close intermolecular associations. C18DMAAC contained long hydrophobic carbon chains, but due to its low concentration, it was difficult for it to effectively exert hydrophobic association at low temperatures, and it could not promote the aggregation of molecular chains by bringing them closer together. Although the polarity and solubility of NVP helped to stretch the molecular chains, at low concentrations, the effect of enhancing intermolecular interactions was limited. When the temperature rose, the thermal motion of molecules increased, and the originally weak intermolecular forces became more difficult to maintain stability. The movement of molecular chains became more free, the concentration of the solution decreased, and the apparent viscosity decreased. For example, at 0.2% by mass, 134 °C became a critical point where the thermal motion of molecules broke the stable structure of the solution. Once the temperature exceeded this value, the viscosity decreased significantly [31]. At 0.4% by mass, between 80 °C and 150 °C, although there was an increase in the thermal motion of molecules, more weak interactions such as hydrogen bonding may form between AM and AMPS, causing a temporary upward trend in viscosity [32]. However, after 150 °C, thermal motion became dominant, and the viscosity decreased again.

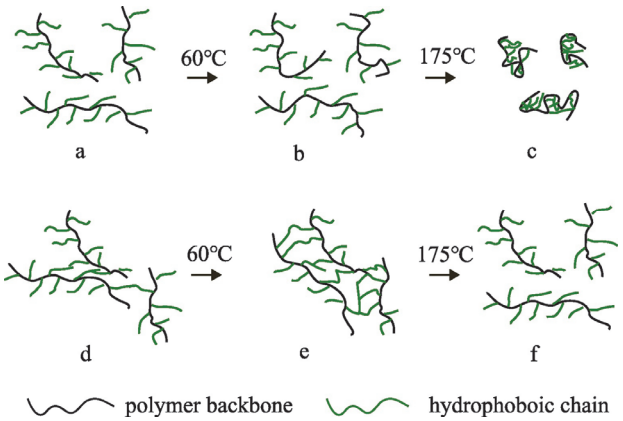


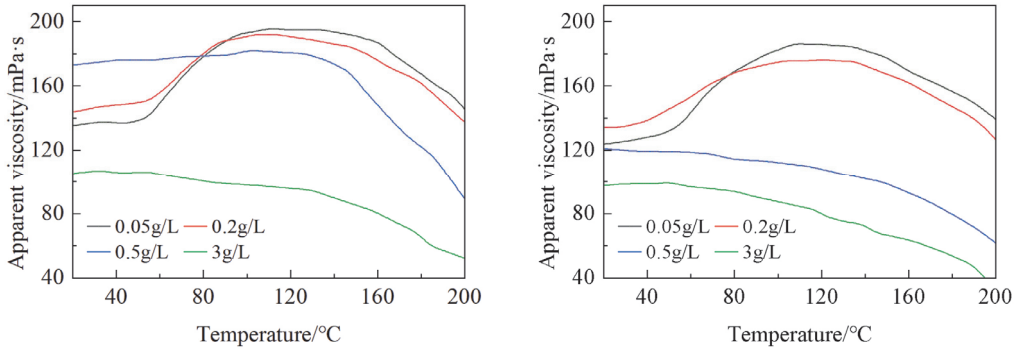
Figure 9. Schematic diagram of the mechanism of polymer structure change with temperature (**a**–**f**).

In contrast, for the polymer in the high-quality fraction state, at high-quality fractions (0.6% and 0.8%), the polymer molecules were densely distributed in the solution, with a small intermolecular distance. The long hydrophobic carbon chain of C18DMAAC played an important role at this time, and a certain degree of hydrophobic association already existed between molecules at lower temperatures (Figure 9d–f), which became more pronounced as the temperature increased. Simultaneously, the temperature-sensitive groups within the polymer experienced a phase transformation from a hydrophilic condition to a hydrophobic one during the medium-temperature stage, which further promoted the hydrophobic association between molecular chains [33]. These effects caused a large number of physical cross-linking points to form between molecular chains, different molecular chains were connected to each other, the movement of molecular chains was greatly restricted, and the fluidity of the solution was significantly reduced, resulting in a rapid increase in viscosity [34]. In addition, due to the high concentration of molecular chains, the chances of collisions and interactions between molecules increased significantly, allowing the hydrophobic association to proceed more fully. During the high-viscosity plateau stage (125–175 °C), the hydrophobic association between molecular chains reached equilibrium, and a relatively stable structure was formed, and the viscosity entered the high-viscosity plateau. Furthermore, the higher the mass fraction and the greater the concentration of molecular chains, the stronger the hydrophobic association, and the wider the temperature range and the higher the upper limit corresponding to the high-viscosity plateau. When the temperature exceeded 175 °C and entered the high-temperature stage, although the thermal motion was intense, the large number of intermolecular action bases at high concentrations could maintain a certain physical cross-linked structure, even if some of the cross-linked structures between molecular chains were destroyed [35]. This explained why the apparent viscosities of TTSTC with mass fractions of 0.6% and 0.8% were still not lower than the values at 20 °C, even when the temperature reached 200 °C.

3.2.3. Salt Tolerance

The change in the apparent viscosity of TTSTC solutions at NaCl concentrations of 0.05 g/L, 0.2 g/L, 0.5 g/L, and 3.0 g/L was studied (Figure 10a). In the low-salt-concentration region (0.05 g/L and 0.2 g/L NaCl), the polymer exhibited the best temperature-sensitive thickening properties in this concentration range, which was manifested by the relatively low initial viscosity (135–143 mPa·s). The sulfonic acid group, located on the AMPS unit, exerted an electrostatic repulsion effect, thereby maintaining the polymer chains in an extended conformation [36]. At temperatures of approximately 60 °C, there was a substantial increase in apparent viscosity, accompanied by a notable temperature-sensitive thickening effect. The temperature-sensitive thickening behavior was ascribed to a moderate ionic strength. This ionic strength neither impacted the equilibrium of electrostatic repulsion nor obstructed the formation of hydrophobic associations [37]. In the medium-salt-concentration region (0.5 g/L NaCl), the polymer exhibited the following characteristics: the initial viscosity at room temperature was higher than that under low-salt-concentration conditions, which was about 173 mPa·s. This was because the moderate ion-shielding effect weakened the electrostatic repulsion and promoted initial association. The increase in viscosity at elevated temperatures was significantly smaller than that under low-salt-concentration conditions, indicating that the temperature-sensitive thickening effect was suppressed. This phenomenon reflected the negative impact of ion shielding on temperature-sensitive performance, and premature association of molecular chains limited further temperature response. In the high-salt-concentration region (3 g/L NaCl), the temperature-sensitive thickening performance was significantly reduced due to the high salt concentration: the viscosity at room temperature was lower than that

under moderate-salt-concentration conditions, at 104 mPa·s, indicating that excessive ion shielding destroyed the original molecular chain association structure [38]. During the temperature rise process, the viscosity gradually decreased, and the temperature-sensitive thickening effect almost disappeared.



(**a**) NaCl (**b**) $CaCl_2$

Figure 10. Effect of variations in NaCl concentration on the viscosity behavior of TTSTC solutions.

Figure 10b demonstrates the changing pattern of apparent viscosity of TTSTC solutions at $CaCl_2$ concentrations of 0.05 g/L, 0.2 g/L, 0.5 g/L, and 3.0 g/L. In the region of low salt concentration, the polymer sheets showed good temperature-sensitive thickening properties, but the apparent viscosity was overall lower than the values in NaCl, where the initial viscosity decreased by 12 mPa·s (for 0.05 g/L salt concentration) and 9 mPa·s (for 0.2 g/L salt concentration), which was attributed to the strong interaction of Ca^{2+} with the sulfonic acid of the AMPS unit. The group interacted more strongly with the AMPS unit, leading to early cross-linking of the polymer chains, which reduced the degree of freedom and initial viscosity. However, at low salt concentrations, $CaCl_2$ provided moderate ionic strength and did not completely inhibit the temperature-sensitive thickening effect. The polymers did not exhibit temperature-sensitive thickening characteristics in both the moderate- and high-salinity-concentration regions, which was attributed to the fact that as the Ca^{2+} concentration increased, the strong ionic cross-linking and excessive ionic shielding disrupted the hydrophobic linkages, resulting in overly tight cross-linking of the polymer chains, which suppressed the response to the temperature change, and the temperature-sensitive thickening effect failed to be observed. Compared with NaCl, $CaCl_2$ introduced stronger Ca^{2+} interactions with the polymer, triggered earlier polymer chain cross-linking, reduced the initial viscosity, and further inhibited the temperature-sensitive thickening behavior at high concentrations.

The experimental results showed that the properties of the AM/AMPS/C18DMAAC/NVP tetrameric temperature-sensitive thickening copolymers were strongly dependent on the salt concentration in solution. The conditions of low concentrations of NaCl and $CaCl_2$ (0.05–0.2 g/L) exhibited the best temperature-sensitive thickening effect, while high concentrations of NaCl (3 g/L) with medium-high concentrations of $CaCl_2$ ($\geq$0.5 g/L) significantly inhibited the temperature-sensitive thickening performance.

3.2.4. Alkali Resistance

The TTSTC solution manifested a relatively stable apparent viscosity with minimal fluctuations when the pH of the solution was within the alkaline range of 11 to 13. This indicated that the copolymer had good stability in a weakly alkaline environment. The stability of the molecular structure was primarily responsible for this phenomenon. Specifically, the sulfonic acid group within the AMPS monomer played a pivotal role. The sulfonic acid group had strong alkali resistance [39] and could maintain a stable chemical state under

weakly alkaline conditions, thereby ensuring the integrity of the polymer molecular chain. In addition, under weakly alkaline conditions, the hydrophobic interaction of the given hydrophobic groups was relatively stable, and the carbonyl group in the NVP structure was not significantly affected; thus, the overall thickening performance of the copolymer was retained (Figure 11).

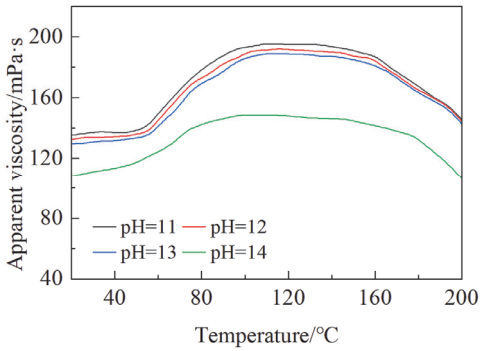


Figure 11. The impact of different pH values on the viscosity characteristics of TTSTC solutions.

However, when the pH of the solution was increased to 14 (highly alkaline conditions), the manifested viscosity of the polymer solution began to decrease significantly. This phenomenon could be attributed to the chemical instability of some functional groups in the polymer molecules. In a highly alkaline environment, the amide group in the AM unit was prone to alkaline hydrolysis [40], generating carboxylates and amino groups. This chemical reaction had the potential to disrupt the molecular chain structure of the polymer, thereby enhancing its flexibility and weakening its intermolecular interactions and particularly its bonding between hydrophobic groups. In addition, alkaline hydrolysis may also reduce the overall network-forming ability of the polymer chain, thereby significantly weakening its thickening properties. From the perspective of the overall stability of the system, the sulfonic acid group in the AMPS unit retained its chemical stability within the weak alkaline and medium alkaline ranges. This was of great significance in supporting the properties of the polymer. The long-chain hydrophobic groups of C18DMAAC were not significantly disturbed in the pH range of 11–13, and their hydrophobic association was an important factor in maintaining the temperature-sensitive thickening performance. The NVP unit, as a non-ionic monomer, had good tolerance of alkaline environments due to its strong chemical stability. Conversely, the amide group in the AM unit acted as a weak link in the stability of the system. It was susceptible to hydrolysis under highly alkaline conditions, a phenomenon that could result in a significant decrease in system performance. Overall, the TTSTC system met the performance requirements of the cementing process (pH = 11–13).

3.3. Influence of Polymers on the Properties of Cement Slurries

3.3.1. Sedimentation Stability

The maximal density variance (MDD) existing between the upper and lower components of the cement slurry and the mass fraction of free liquid were analyzed upon the addition of 0, 0.2%, 0.4%, 0.6%, 0.8%, and 1.0% temperature-sensitive thickeners to the cement slurry, as depicted in Figure 9. The experiment was conducted under conditions of elevated temperature and pressure, with a temperature of 155 °C and a pressure of 95 MPa. The cement slurry without added polymer exhibited a large difference in upper and lower density and a high mass fraction of free liquid, indicating severe sedimentation instability and liquid phase separation in the slurry. As the quantity of polymer added to the cement slurry increased, the disparity in upper and lower density diminished gradually,

concomitantly with a substantial decrease in the mass fraction of free liquid. Upon reaching a polymer addition rate of 0.6%, the variation in upper and lower densities of the cement slurry was regulated to within 0.03 g/cm^3. Concurrently, the mass fraction of free liquid was minimized to the lowest level, thereby satisfying the stringent requirements of on-site construction. The primary rationale for this phenomenon pertained to the thickening effect of the polymer at elevated temperatures. Initially, it elevated the viscosity and the internal structural force of the cement slurry, which effectively suppressed the settlement of cement particles. Second, the formation of a three-dimensional network structure and the adsorption of free water enhanced the overall stability of the cement slurry (Figure 12).

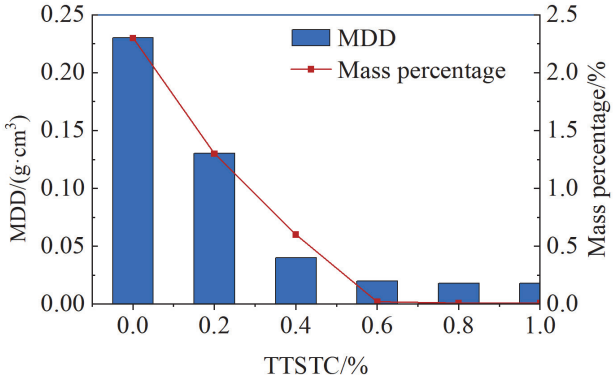


Figure 12. The maximum density difference and the mass proportion of free liquid in the cement slurry under different proportions of thermosensitive thickeners.

3.3.2. Thickening Properties

From the experimental data (Figure 13), it can be seen that after the addition of a temperature-sensitive thickener to the cement slurry system, the thickening time changed from 4.47 h to approximately 4.88 h. Nevertheless, this extended time was still within a reasonable range for cementing operations. In addition, the incorporation of 0.6% TTSTC into the cement slurry ensured the stability of the slurry system throughout the experimental phase, with no significant variations. In contrast, when no TTSTC was added, the consistency of the slurry system decreased significantly to approximately 6Bc after approximately 1 h. At 4.5 h, the consistency of the cement paste system with xanthan gum thickener was 10.75 Bc, which was 55.7% lower than the 0 h consistency, while the consistency of the cement paste with TTSTC reagent was 19.29 Bc, which was 24.8% lower than the 0 h consistency, and the reduction in consistency compared with that of the control group was 30.9%, which further provided a strong argument for the good thickening effect of TTSTC. This result further provided strong experimental evidence that TTSTC had a good thickening effect.

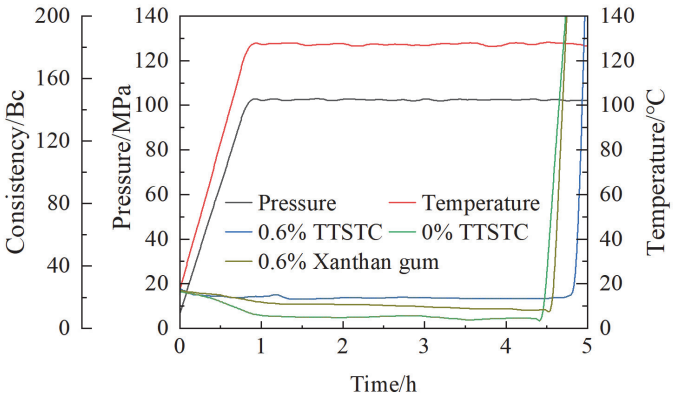


Figure 13. The thickening curve of cement slurry.

3.3.3. Compressive Strength of Cement Paste

As illustrated in Figure 14, in the initial phase of cement hydration (3d), the compressive strength exhibited a decline in conjunction with the augmentation of the mass fraction of the thickener. This was because in the early stage of cement hydration, hydrophilic groups such as AM and AMPS would adsorb a large number of water molecules to form a hydration film on the surfaces of cement particles [41]. This hydration film would prevent the direct contact between cement particles and water, slowing down the hydration reaction rate of cement. At the same time, the long-chain alkyl groups had a certain steric hindrance effect, which could interfere with the mutual collision and aggregation of cement particles [42], inhibiting the formation and growth of cement hydration products. It was difficult to quickly form a cementitious stone structure with strength, resulting in a decrease in early strength of the cementitious stone.

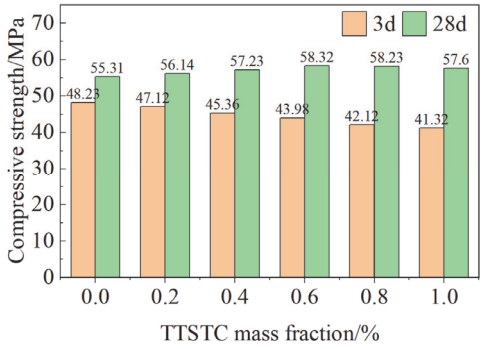


Figure 14. The compressive strengths of cement stones with different mass fractions of TTSTC.

After a 28-day hydration period, the compressive strength of the cement paste exhibited an initial increase, followed by a subsequent decrease in conjunction with the escalating mass fraction of the thickener. The maximum compressive strength was 58.23 MPa at a mass fraction of 0.6%. This phenomenon could be attributed to the critical function of the temperature-sensitive thickener in optimizing the pore structure of the cement paste. Due to the thickening effect and adsorption properties of the copolymer, a more uniform density in the cement paste system was ensured, thereby reducing the formation of large pores in the cement paste formation [43] and reducing the porosity. The presence of the copolymer promoted the uniform precipitation of hydration products, resulting in an increased proportion of microporous structures and thus improved densification of the cement paste.

From a microscopic point of view, when the mass fraction of the thermosensitive thickener exceeded 0.6%, the excessive copolymer molecules aggregated with each other, and the excessive C18-DMAAC long-chain alkyl groups created excessive steric hindrance, which seriously hindered the further hydration reaction process of cement particles and led to insufficient production of hydration products in the later stage. From a macroscopic point of view, this not only destroyed the original optimization effect on the pore structure but also formed stress concentration points inside the cement paste, while blocking the chemical bonding between cement hydration products, reducing the internal structural connection strength of the cement paste, which could not effectively resist external forces, and ultimately leading to a decrease in strength. However, the compressive strength of the cement slurry system at 28d for the mass fraction involved in the experiment met the requirements of on-site construction.

3.3.4. Hydration Kinetics Analyses Results

Figure 15 shows the total exothermic curves of cement paste systems containing different mass fractions of TTSTC over a period of 90 h. From the curves, it can be seen that

when the content of TTSTC in the cement paste is 0%, 0.2%, 0.4%, 0.6%, 0.8% and 1%, the main exothermic times are 0–12 h, 1–13 h, 2–14h, 3–15 h, 4–16 h and 5–17 h, and the total exothermic quantities in 90 h were 413.5 J/g, 389.2 J/g, 370.0 J/g, 350.9 J/g, 333.8 J/g, and 315.6 J/g, respectively. This further confirmed that the decrease in early cementite strength with the increase in TTSTC content in Section 3.3.3 was related to the degree of hydration and that the adsorption of water molecules by hydrophilic groups, such as AM, AMPS, etc., to form a hydration film on the surface of the cement particles and the spatial resistance of the long-chain alkyl groups in C18DMAAC were responsible for the decrease in early hydration. This effect was the main reason for the reduction in early hydration degree. At a TTSTC mass fraction of 1.0%, the main time of hydration exotherm was delayed by about 14 h compared with that of the cement paste system without TTSTC, which met the performance requirements of the cement paste system in the cementing process.

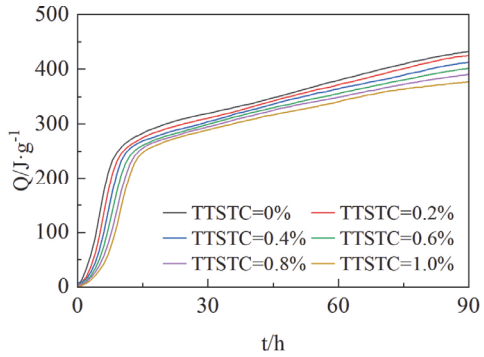


Figure 15. Total heat release curve of cement paste with different contents of TTSTC.

4. Conclusions

(1) The target polymer TTSTC was successfully synthesized by aqueous solution radical polymerization using AM, AMPS, long-chain C18DMAAC, and NVP as monomers. The polymerization conditions were optimized by orthogonal experiments, and the optimal monomer molar ratio was determined to be 15:10:5:5, the initiator concentration was 16 wt%, the cross-linking agent concentration was 0.45 wt%, the pH was 6, and the polymerization temperature was 60 °C.

(2) In-depth characterization of the chemical structure of TTSTC using Fourier transform infrared spectroscopy (FT-IR), proton nuclear magnetic resonance (^{1}H-NMR), gel permeation chromatography, scanning electron microscopy (SEM), Zeta potential, and particle size tests confirmed the successful synthesis of the target polymer and validated its molecular structural properties containing thermosensitive monomers and functional groups.

(3) TTSTC demonstrated remarkable thermosensitive thickening properties under elevated temperatures (up to 279 °C) and high alkaline conditions (pH 11–13) and was stable in a saline environment with a NaCl/$CaCl_2$ concentration of 0.05–0.5 g/L. The thickening performance of TTSTC was optimal when the mass fraction was 0.6–0.8 wt%.

(4) The incorporation of TTSTC was demonstrated to enhance the sedimentation stability of the cement slurry, thereby mitigating the risk of delamination under elevated temperatures and promoting enhanced slurry homogeneity.

(5) The compressive strength of the cement stone was significantly increased with the addition of TTSTC at 0.6–1.0 wt%. The experimental results showed that TTSTC could effectively improve the 28d mechanical properties of cementite with less influence on the hydration kinetics, which provided a reliable guarantee for the integrity of the wellbore under a high-temperature and high-pressure environment.

This study focused mainly on the optimization of the synthesis conditions, the characterization of the chemical structure of TTSTC, and its effectiveness in the application of cement paste systems, while the potential for its application in other fields or more complex environments needs to be further explored. In addition, the long-term stability and environmental friendliness of TTSTC need to be further evaluated. Future research directions will aim to expand the application areas of TTSTC, explore its performance under other extreme conditions, and optimize its environmental friendliness to meet more diversified application needs.

Author Contributions: X.C., investigation, methodology, and writing—original draft. X.Z., formal analysis and writing—original draft. C.G., data curation and writing—original draft. Y.L., resources and writing—original draft. D.L., conceptualization and writing—review and editing. All authors have read and agreed to the published version of the manuscript.

Funding: This research received no external funding.

Data Availability Statement: No new data were created or analyzed in this study.

Conflicts of Interest: Author Xiangpeng Zhu was employed by the company The Second Cementing Division of the CNPC Bohai Drilling Engineering Company Limited. Author Cheng Gan was employed by the NO.1 Drilling Engineering Company of CNPC Bohai Drilling Engineering Company Limited. Author Yigang Li was employed by the CNPC Bohai Drilling Engineering Company Limited. The remaining authors declare that the research was conducted in the absence of any commercial or financial relationships that could be construed as a potential conflict of interest. The The Second Cementing Division of the Bohai Drilling and Exploration Company, BHDC and CNPC Bohai Drilling Engineering Company Limited had no role in the design of the study; in the collection, analyses, or interpretation of data; in the writing of the manuscript, or in the decision to publish the results.

References

1. Li, P.; Wang, L.; Lai, X.; Gao, J.; Dang, Z.; Wang, R.; Mao, F.; Li, Y.; Jia, G. Two-Level Self-Thickening Mechanism of a Novel Acid Thickener with a Hydrophobic-Associated Structure during High-Temperature Acidification Processes. *Polymers* **2024**, *16*, 679. [CrossRef] [PubMed]
2. Fakher, S.; El-Sayed, A.; Sameh, L.; Abdeltawab, B. Evaluating a Novel Fly Ash Resin-Reinforced Cement's Interactions under Acidic, Basic, High-Salinity, and High-Temperature Conditions. *Polymers* **2023**, *15*, 3404. [CrossRef] [PubMed]
3. Feng, Q.; Jia, F.; Peng, Z.; Zheng, Y. Development of temperature-responsive suspension stabilizer and its application in cementing slurry system. *Colloids Surf. A Physicochem. Eng. Asp.* **2023**, *658*, 130734. [CrossRef]
4. Wang, Z.; Sun, J.; Huang, X.; Lv, K.; Geng, Y. A temperature-sensitive polymer with thinner effect as a rheology modifier in deepwater water-based drilling fluids. *J. Mol. Liq.* **2024**, *393*, 123536. [CrossRef]
5. Wang, R.; Zhu, Z.; Su, X.; Mianowicz, K.; Jia, H.; Wu, K. Slurry pumps in deep-sea mining: A review of numerical and experimental studies. *Ocean Eng.* **2022**, *251*, 111150. [CrossRef]
6. Zhou, P.; Li, M.; Zhang, C.; Xia, X.; Yu, Y.; Qi, F.; Wu, Y. Ultra-high temperature suspending stabilizer and cement slurry interface interaction law and mechanism study for ultra-deep well cementing. *Constr. Build. Mater.* **2023**, *409*, 133979. [CrossRef]
7. Lv, K.; Huang, Z.; Ling, X.; Xia, X. Analysis of the weight loss of high temperature cement slurry. *Fluid Dyn. Mater. Process.* **2022**, *18*, 1307–1318. [CrossRef]
8. Djouonkep, L.D.W.; Xie, B.; Tao, H.; Zhuo, L.; Tchameni, A.P.; Zhao, L. Investigating the structure-to-property of thermo-thickening polymers capped by different structural side chains. *React. Funct. Polym.* **2023**, *186*, 105569. [CrossRef]
9. Chen, F.; Lu, G.; Yuan, H.; Li, R.; Nie, J.; Zhao, Y.; Shu, X.; Zhu, X.; Chen, F. Mechanism and regulation of LCST behavior in poly(hydroxypropyl acrylate)-based temperature-sensitive hydrogels. *J. Mater. Chem. A* **2022**, *10*, 18235–18247. [CrossRef]
10. Bai, X.; Yong, X.; Luo, Y.; Deng, L.; Li, K.; Zhou, Y. Synthesis and application of temperature-sensitive polymer as a novel plugging agent for water-based drilling fluids synthesis and application of temperature-sensitive polymer as a novel plugging agent for water-based drilling fluids. *J. Appl. Polym. Sci.* **2022**, *139*, e52524. [CrossRef]
11. Yang, G.; Liu, T.; Zhu, H.; Zhang, Z.; Feng, Y.; Leusheva, E.; Morenov, V. Heat control effect of phase change microcapsules upon cement slurry applied to hydrate-bearing sediment. *Energies* **2022**, *15*, 4197. [CrossRef]
12. Cai, W.; Deng, J.; Luo, M.; Feng, Y.; Li, J.; Liu, Q. Recent advances of cementing technologies for ultra-HTHP formations. *Int. J. Oil Gas Coal Technol.* **2022**, *29*, 27–51. [CrossRef]

13. Feng, J.; Zheng, L.; Wu, X.; Wu, J.; Yu, Y.; Li, L.; Li, M. Preparation and characterization of polymer retarder for plugging cement slurry. *J. Dispers. Sci. Technol.* **2023**, *44*, 2239–2246. [CrossRef]
14. Zou, Q.; Chen, X.; Zhong, S.; Yi, D.; Liu, L. Performance experiment of ultra high temperature cementing slurry system. *Front. Mater.* **2024**, *11*, 1383286. [CrossRef]
15. Shi, J.; Wu, Z.; Deng, Q.; Liu, L.; Zhang, X.; Wu, X.; Wang, Y. Synthesis of hydrophobically associating polymer: Temperature resistance and salt tolerance properties. *Polym. Bull.* **2022**, *79*, 4581–4591. [CrossRef]
16. Hou, Y.; Guo, Y.; Qian, S.; Khan, H.; Han, G.; Zhang, W. A new thermoresponsive polymer of poly(N-acetoxylethyl acrylamide). *Polymer* **2019**, *167*, 159–166. [CrossRef]
17. Papadakis, C.M.; Niebuur, B.-J.; Schulte, A. Thermoresponsive polymers under pressure with a focus on poly (n-isopropylacrylamide) (pnipam). *Langmuir* **2023**, *40*, 1–20. [CrossRef]
18. Wang, W.; Gao, C.; Qu, Y.; Song, Z.; Zhang, W. In Situ Synthesis of Thermoresponsive Polystyrene-b-poly(N-isopropylacrylamide)-b-polystyrene Nanospheres and Comparative Study of the Looped and Linear Poly(N-isopropylacrylamide)s. *Macromolecules* **2016**, *49*, 2772–2781. [CrossRef]
19. Li, J.; Wen, M.; Jiang, Z.; Gao, S.; Xiao, X.; Xiang, C.; Tao, J. Formulation and characterization of surfactants with antibacterial and corrosion-inhibiting properties for enhancing shale gas drainage and production. *Sci. Rep.* **2025**, *15*, 2376. [CrossRef]
20. Yan, Y.; Xue, Z.; Wu, L.; Luo, Y.; Bai, X. Synthesis and application of a temperature sensitive poly (acrylamide-co-n-isopropylacrylamide-co-sodium p-styrene sulfonate) as a new water-based drilling fluid plugging agent. *J. Appl. Polym. Sci.* **2025**, e56733. [CrossRef]
21. Ran, Y.; Zhang, G.; Jiang, P.; Pei, H. Preparation method and performance evaluation of a gel based on am/amps copolymer. *Gels* **2022**, *8*, 802. [CrossRef]
22. Przesławski, G.; Szcześniak, K.; Gajewski, P.; Marcinkowska, A. Influence of Initiator Concentration on the Polymerization Course of Methacrylate Bone Cement. *Polymers* **2022**, *14*, 5005. [CrossRef] [PubMed]
23. Guo, J.; Dong, M.; Yu, Y. Synthesis and property of thermo-thickening oil well cement additives. *J. Tianjin Univ. Sci. Technol.* **2016**, *49*, 597–602.
24. Majumder, L.; Bera, K.; Khamaru, K.; Pal, U.; Maiti, N.C.; Banerji, B. NMR and vibrational spectroscopic studies on the structure and self-assembly of Two de novo dipeptides in methanol. *J. Mol. Struct.* **2022**, *1266*, 133455. [CrossRef]
25. Shi, S.; Sun, J.; Lv, K.; Liu, J.; Bai, Y.; Wang, J.; Huang, X.; Jin, J.; Li, J. Comparative studies on thickeners as hydraulic fracturing fluids: Suspension versus powder. *Gels* **2022**, *8*, 722. [CrossRef]
26. Zhang, D.; Zhang, M.; Luo, Z.; Zhang, S. Design, synthesis, and characterization of novel copolymer gel particles for water-plugging applications. *e-Polymers* **2024**, *24*, 20240016. [CrossRef]
27. Wang, Q.; Zhou, C.; Zhang, H.; Zhang, X.; Wen, X.; Bai, J.; Mao, H. Preparation of low-molecular-weight polyacrylamide as the delayed crosslinking plugging agent for drilling fluid. *Gels* **2024**, *10*, 112. [CrossRef]
28. Wang, C.; Wang, H.; Xue, Y.; Yang, L.; Wang, R.; Jin, J.; Li, Y. Development and performance of thermo-viscosifying polymer for high temperature sedimentation control of high density cement slurry. *Acta Pet. Sin.* **2020**, *41*, 1416.
29. Wu, Y.; Duan, M.; Wang, Q.; Chen, B.; Chen, H.; Li, X.; Fang, S. Dispersion polymerization of am-amps-dam-doh and its sand control property. *Geoenergy Sci. Eng.* **2024**, *241*, 213190. [CrossRef]
30. Li, J.; Wen, M.; Jiang, Z.; Xian, L.; Liu, J.; Chen, J. Development and characterization of a surfactant responsive to redox conditions for gas recovery in foam drainage. *Sci. Rep.* **2025**, *15*, 511. [CrossRef]
31. Xiaolin, L.; Jianhua, L.; Hongbin, Y.; Wenming, L.; Ben, Q.; Zhe, L.; Jingyu, Y. Study on thermally viscosifying copolymer as a high temperature stabilizer for high density cement slurries. *Drill. Fluid Complet. Fluid* **2022**, *39*, 76–81.
32. Reddy, B.R.R.; Patil, R.; Patil, S. Chemical modification of biopolymers to design cement slurries with temperature-activated viscosification—A laboratory study. *SPE Drill. Complet.* **2012**, *27*, 94–102. [CrossRef]
33. Tchameni, A.P.; Xie, B.; Zhang, H.; Zhao, L.; Luo, M.; Wen, J. Thermo-associating polymers based on cross-linked 2-acrylamido-methylpropane sulfonic acid, Part A: Synthesis and solution behavior. *Colloids Surf. A Physicochem. Eng. Asp.* **2020**, *593*, 124611. [CrossRef]
34. Su, X.; Feng, Y. Thermoviscosifying smart polymers for oil and gas production: State of the art. *ChemPhysChem* **2018**, *19*, 1941–1955. [CrossRef]
35. Chen, X.; Wang, C.; Wang, Y.; Wang, H.; Wang, R. Prevention strategy of cement slurry sedimentation under high temperature. Part 1: A polymer with continuous thermo-thickening behavior from 48 to 148 C. *J. Phys. Chem. C* **2019**, *123*, 18573–18584. [CrossRef]
36. Xu, S. Research progress on viscosity reducing agents for water-based drilling fluids. *Stand. Qual. China's Pet. Chem. Ind.* **2023**, *43*, 99–101.
37. Liu, Y.; Huang, X.; Zhang, X.; Dai, Z.; Li, T. Study on temperature and salt resistance plugging agent and characterization of its structure. *Appl. Chem. Ind.* **2023**, *52*, 3392–3396. [CrossRef]
38. Li, J.; Wen, M.; Yang, J.; Liu, Y.; Jiang, Z.; Chen, J. Synthesis and analysis of magnetic nanoparticles within foam matrix for foam drainage gas production. *Geoenergy Sci. Eng.* **2024**, *238*, 212887. [CrossRef]
39. Xie, S.; Zhang, J.; Lin, R.; Wang, J.; Zhu, H.; Xie, Y. Analysis on retarding effect of amps retarder at high temperature. *Contemp. Chem. Ind.* **2024**, *53*, 1–6. [CrossRef]

40. Luo, Y.; Lin, L.; Guo, Y.; Luo, P.; Xiong, G.; Li, Z.; Ao, H. Study on high-temperature degradation of acrylamide-based polymer ZP1 in aqueous solution. *Polym. Degrad. Stab.* **2023**, *217*, 110533. [CrossRef]
41. Lai, X.; Liu, G.; Liu, Y.; Dong, X.; Liu, X.; Mukhtar, Y.; Wang, L.; Wen, X.; Lu, L. Preparation and viscoelasticity of novel hydrophobic associating polymer with salt stimulation responsiveness by functional monomer modification for fracturing fluids. *Colloid Polym. Sci.* **2023**, *301*, 1271–1283. [CrossRef]
42. Wu, L.; Zhao, B.; Hou, W.; Shi, L.; Dong, Z.; Zou, S. Research progress of oil well cement suspension. *Oilfield Chem.* **2023**, *40*, 736–742. [CrossRef]
43. Shang, L. Research on quality evaluation methods of ultra-low density cementing in oil well cementing. *Petrochem. Ind. Technol.* **2024**, *31*, 215–217.

Disclaimer/Publisher's Note: The statements, opinions and data contained in all publications are solely those of the individual author(s) and contributor(s) and not of MDPI and/or the editor(s). MDPI and/or the editor(s) disclaim responsibility for any injury to people or property resulting from any ideas, methods, instructions or products referred to in the content.